

Stability Evaluation of a Fixed-Wing Unmanned Aerial Vehicle with Morphing Wingtip

Tuğrul Oktay¹ , Yüksel Eraslan^{2*} 

¹Erciyes University, Faculty of Aeronautics and Astronautics, Kayseri, Türkiye. (oktay@erciyes.edu.tr).

^{2*}İskenderun Technical University, İskenderun Vocational School of Higher Education, Hatay, Türkiye. (yuksele.eraslan@iste.edu.tr).

Article Info

Received: February, 14. 2022

Revised: April, 29. 2022

Accepted: May, 06. 2022

Keywords:

Unmanned aerial vehicle

Morphing wingtip

Aerodynamics

Stability

Autonomous control

Corresponding Author: *Yüksel Eraslan*

RESEARCH ARTICLE

<https://doi.org/10.30518/jav.1073417>

Abstract

Aeronautical applications of morphing technologies are continued to increase their popularity and wide spread application during last years. The technology takes place in not only military, but also civil applications that aims providing superior performances to manned or unmanned aircraft than conventional configurations. However, multidisciplinary approach is required for an aerial vehicle to have ultimate outcome from such an application due to existence of interdisciplinary interactions. Therefore, this research aims to investigate effects of morphing wingtip application on longitudinal and lateral-directional stabilities of a fixed-wing unmanned aerial vehicle, which have remarkable effect on autonomous control performance considerations. In this article, morphing wingtip refers to folding the wing from a determined spanwise location with a dihedral angle. With the aim of the study, wingtips of an unmanned aerial vehicle were folded with 15, 30 and 45 degrees of dihedral angles to be compared with original non-dihedral design. Longitudinal and lateral-directional characteristics of new variations were evaluated in terms of stability derivatives by means of linearized equations of motion that were also presented in state-space representation. Aerodynamic impacts of each variation were assessed by means of computational results obtained from analyses with three-dimensional panel method. Furthermore, taking inertial changes into consideration, concluding remarks on both longitudinal and lateral-directional stability derivatives were presented for each configuration.

1. Introduction

In the last decades, increasing popularity of unmanned aerial vehicles (UAV) in both military and civil applications led scientists to spend further effort on performance enhancement of these vehicles (Konar et al. 2020). Both of fixed-wing and rotary-wing UAVs have their own pros and cons depending on operational purposes. For instance, while rotary-wing configurations have superior ability in hovering flight, fixed-wing configurations are capable of flying at higher altitudes and airspeeds with extended range and endurance (Konar, 2020).

One of the most recent and popular approaches are morphing applications on appropriate components of aircraft, such as wing, tail or fuselage (Sofla et al., 2010). Rather than traditional applications of control-aimed surface deflections, i.e. aileron, rudder, elevator etc., the term “morphing” refers geometrical change in any part of the aircraft to improve its aerodynamic or related disciplinary performances. The application is entitled as active or passive with respect to taking place in-flight or not, respectively (Kose et al., 2020).

Wings can be proposed as suitable for morphing applications on fixed-wing UAVs, as a major lifting surface

and significant source of drag in aerodynamic manner. Lift force generation of a wing is strongly related with its sectional and planform shape, air density and airspeed, thus changing the design of the wing will be resulted in alteration of amount or spanwise distribution of lift force. On the other hand, drag force of an aircraft comprises of parasitic and induced drag components, which are also related with shape of the wing. Therefore, target performance oriented suitable adjustment of aerodynamic forces on an aircraft can be possible with changing its shape via morphing applications. For instance, induced drag relates with wing-tip vortices and generally designers make an effort to eliminate this unfavorable effect via wing-tip devices such as winglets (Yen et al., 2011). In a similar manner, additional to aerodynamics; stability, control or structural performances of an UAV can be improved via morphing wing applications (Oktay et al., 2016, Çoban, 2019, Konar, 2019). However, in order to have an effective thriving outcome for a vehicle, usually, multidisciplinary approach is required because of forecasted interdisciplinary interactions.

Autopilots are frequently used on UAVs with the purpose of guiding the vehicle without necessity for pilot assistance. This autonomous control performance is a considerable issue for UAVs and dramatically relates with shape of the main

wing that is the most important component of an aircraft in terms of aerodynamics (Oktay et al., 2018, Kose et al., 2021). Therefore, improvement of the autonomous performance can also be possible with suitable morphing applications, theoretically. Nevertheless, in order to evaluate effects of morphing technologies on autonomous control performance, it is essential to investigate stability of the aircraft which is interpreted in longitudinal, lateral and directional axes separately (Çoban, 2020). While longitudinal stability is associated with pitching motion, lateral and directional stabilities are related with roll and yaw motions, respectively. In order to investigate each motional characteristics, it is essential to evaluate aircraft equations of motion and eventually constitute longitudinal and lateral parametric state-space models. The state-space models include stability derivatives, inertial considerations and flight condition related terms (Çelik et al., 2016). Therefore, for same flight condition, as morphing application leads to different aerodynamic and inertial characteristics, they should also be investigated. Moreover, morphing related aerodynamic and geometrical alterations of an aircraft lead to change in stability derivatives and correspondingly stability of the vehicle (Kanat et al., 2019). For the purpose of investigating effects of morphing application on aerodynamic characteristics of vehicle, numerical investigation methods, such as Computational Fluid Dynamics, generally considered as proper rather than expensive experimental setups (Şumnu et al., 2021, Oktay et al. 2021).

In the recent past, there are various studies aiming investigation of aerodynamics and stability derivatives of aerial vehicles in analytical, numerical or experimental manner in the literature. A study on a transport aircraft with flared-hinge folding wingtips was shown that the folding has a little effect on longitudinal flight dynamic modes, but excessive alteration on lateral-directional dynamic modes due to generated larger drag forces (Ajaj, 2021). Implications in the article about corresponding stability and control derivatives of the aircraft were provided via aerodynamic results taken from analyses carried out with computational application of vortex lattice method. In another study, effect of in-flight folding wingtip application on aircraft roll dynamics in terms of roll damping and aileron effectiveness was assessed depending on varying wingtip size and folding angle (Dussart et al., 2019). The results were presented with respect to upward and downward deflection rates of wingtips. On the other hand, a study was investigated aerodynamic effects of morphing wingtip application in terms of both twist and dihedral angles by means of both computational and experimental approaches (Smith et al., 2014). A blended-wing-body aircraft was investigated in terms of static and dynamic stability together with taking airworthiness regulations into consideration (Lixin et al., 2022). Long range eVTOL aircraft preliminary design was assessed in terms of control and stability issues for each flight phase. With that purpose, a controller was designed with the aim of handling quality improvement. The analytical model was applied to estimate stability derivatives (Schoser et al., 2022).

In this article, stability evaluation of a fixed-wing UAV ZANKA-I was carried out in consideration of wingtip morphing application. The main wing of the vehicle folded with dihedral angles 15, 30 and 45 degrees from approximately 84.7% of its semi-span location. Taking cruise flight conditions into consideration, aerodynamic effects were investigated by means of 3D panel method. Inertial alterations were discussed and related stability derivatives were evaluated. In summary, the effect of morphing wingtip

application with various dihedral angles was evaluated in stability contributions point of view.

2. Material and Method

In this article, morphing wingtip application was investigated on ZANKA-I fixed-wing UAV, given in Figure 1, in terms of effects on longitudinal and lateral stability derivatives. With respect to the objective of the paper, required reference parameters about the vehicle were taken from a previous study in the literature (Oktay et al., 2016). In order to investigate effects of morphing wingtip application on the stability derivatives, it is essential to derive aircraft equations of motion in suitable form and obtain impacts of the morphing on related terms.

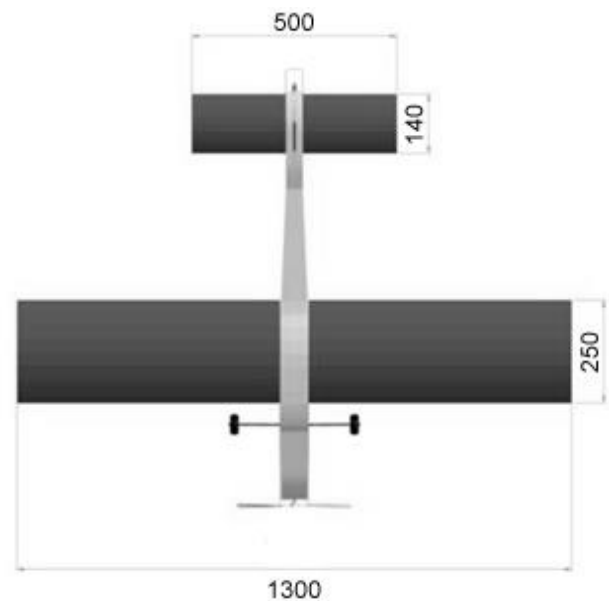


Figure 1. Top-view of ZANKA-I unmanned aerial vehicle with dimensions in mm (Oktay et al., 2016)

2.1. Equations of Motion and State-space Representation

Stability derivatives that previously mentioned are taken place in longitudinal and lateral equations of motion of vehicle. Rigid body equations of motion include force, moment and kinematic equations of the related body. As indicated, autonomous control performance of such an aircraft is dramatically depends on the related equations and so stability derivatives, naturally. The most common representation of these equations were given as parametric state-space model of the aircraft for both longitudinal and lateral approach in Equation 1 and Equation 2, respectively (Nelson, 1998). In these equations, control surface deflections ($\delta_e, \delta_a, \delta_r$), linear velocities (u, v, w), angular velocities (p, q, r), forces (X, Y, Z) and moments (L, M, N) of the vehicle taken place in aircraft frame of reference, as given in Figure 2. On the other hand, there is an impact of certain inertial terms I_x, I_y, I_z and I_{xz} , which are the moments of inertia around the x, y, z axes and xz plane, respectively.

Aircraft equations of motion can be written as first-order differential equations named as state-variable representation that includes aerodynamic and inertial variables, stability derivatives and mass properties of the aircraft as given in Equation 1, where x stands for state vector and η refers to control vector, A and B are the matrices including aircraft dimensional stability derivatives (Nelson, 1998).

$$\dot{x} = Ax + B\eta \quad (1)$$

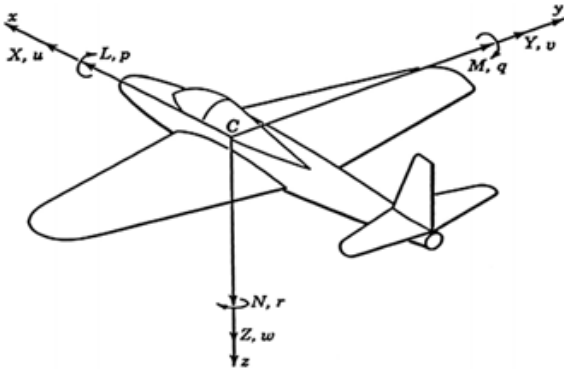


Figure 2. Aircraft body-fixed reference frame and related forces, moments, angular and linear velocities (Deepa et al., 2015)

In compliance with the equation stated above, Equation 2 and Equation 3 are the state-space representation of the aircraft equations of motion in longitudinal and lateral axes, respectively, where θ is pitching angle, ϕ is yawing angle, u is airspeed and g is the gravitational acceleration. Moreover, the subscript “0” refers to reference condition of each term.

$$\begin{bmatrix} \Delta \dot{u} \\ \Delta \dot{w} \\ \Delta \dot{q} \\ \Delta \dot{\theta} \end{bmatrix} = \begin{bmatrix} X_u & X_w & 0 & -g \\ Z_u & Z_w & u_0 & 0 \\ M_u + M_w Z_w & M_w + M_w Z_w & M_q + M_w u_0 & 0 \\ 0 & 0 & 1 & 0 \end{bmatrix} \begin{bmatrix} \Delta u \\ \Delta w \\ \Delta q \\ \Delta \theta \end{bmatrix} \quad (2)$$

$$+ \begin{bmatrix} X_{\delta_r} & X_{\delta_e} \\ Z_{\delta_r} & Z_{\delta_e} \\ M_{\delta_r} + M_w Z_{\delta_r} & M_{\delta_e} + M_w Z_{\delta_e} \\ 0 & 0 \end{bmatrix} \begin{bmatrix} \Delta \delta_r \\ \Delta \delta_e \end{bmatrix}$$

$$\begin{bmatrix} \Delta \dot{v} \\ \Delta \dot{p} \\ \Delta \dot{r} \\ \Delta \dot{\phi} \end{bmatrix} = \begin{bmatrix} Y_v & Y_p & -(u_0 - Y_r) & -g \cos(\theta_0) \\ L_v^* + \frac{I_{xz}}{I_x} N_v^* & L_p^* + \frac{I_{xz}}{I_x} N_p^* & L_r^* + \frac{I_{xz}}{I_x} N_r^* & 0 \\ N_v^* + \frac{I_{xz}}{I_z} L_v^* & N_p^* + \frac{I_{xz}}{I_z} L_p^* & N_r^* + \frac{I_{xz}}{I_z} L_r^* & 0 \\ 0 & 1 & 0 & 0 \end{bmatrix} \begin{bmatrix} \Delta v \\ \Delta p \\ \Delta r \\ \Delta \phi \end{bmatrix} \quad (3)$$

$$+ \begin{bmatrix} 0 & Y_{\delta_r} \\ L_{\delta_a}^* + \frac{I_{xz}}{I_x} N_{\delta_a}^* & L_{\delta_r}^* + \frac{I_{xz}}{I_x} N_{\delta_r}^* \\ N_{\delta_a}^* + \frac{I_{xz}}{I_z} L_{\delta_a}^* & N_{\delta_r}^* + \frac{I_{xz}}{I_z} L_{\delta_r}^* \\ 0 & 0 \end{bmatrix} \begin{bmatrix} \Delta \delta_a \\ \Delta \delta_r \end{bmatrix}$$

2.2. Longitudinal Stability Derivatives

Aircraft longitudinal equations of motion comprise of longitudinal stability derivatives, which are stated as A and B matrices previously, in Equation 2. The derivatives can be divided in two groups as force and moment derivatives that can be estimated from equations that include aerodynamic coefficients, dynamic pressure Q , wing area S , mass m , reference airspeed u_0 , and wing mean aerodynamic chord length \bar{c} (Nelson, 1998).

Longitudinal stability derivatives of X-force and Z-force are X_u , X_w , Z_u and Z_w , which refers to variations in forces in terms of linear velocities u and w . Impact of reference drag

coefficient C_{D_0} on derivative X_u can be clearly seen from Equation 4. Moreover, drag curve slope C_{D_α} and reference lift coefficient C_{L_0} have remarkable effect on X_w , as given in Equation 5. Similarly, Equation 6 and Equation 7 evidently reveals that Z-force derivatives Z_u and Z_w are directly affected from reference lift coefficient, lift curve slope C_{L_α} and reference drag coefficients of the aircraft.

$$X_u = \frac{(-C_{D_\alpha} - 2C_{D_0})QS}{mu_0} \quad (4)$$

$$X_w = \frac{-(C_{D_\alpha} - C_{L_0})QS}{mu_0} \quad (5)$$

$$Z_u = \frac{-(C_{L_\alpha} + 2C_{L_0})QS}{mu_0} \quad (6)$$

$$Z_w = \frac{-(C_{L_\alpha} + C_{D_0})QS}{mu_0} \quad (7)$$

Moments point of view, derivatives of M_u , M_w , $M_{\dot{w}}$ and M_q give brief idea about effects of linear velocities u and w , angular rate \dot{w} and angular velocity q on pitching moment variations, respectively. Different from force derivatives, estimation of moment derivatives requires also y-axis moment of inertia I_y . Equations given below include also various pitching moment coefficient related terms C_{m_u} , C_{m_α} , $C_{m_{\dot{\alpha}}}$, and C_{m_q} , which suggest information about variation in pitching moment coefficient with linear velocity u , angle of attack α , rate of angle of attack $\dot{\alpha}$, and angular velocity q .

$$M_u = C_{m_u} \frac{(QSc)}{u_0 I_y} \quad (8)$$

$$M_w = C_{m_\alpha} \frac{(QSc)}{u_0 I_y} \quad (9)$$

$$M_{\dot{w}} = C_{m_{\dot{\alpha}}} \frac{\bar{c} (QSc)}{2u_0 u_0 I_y} \quad (10)$$

$$M_q = C_{m_q} \frac{c QSc}{2u_0 I_y} \quad (11)$$

2.3. Lateral-Directional Stability Derivatives

In order to have lateral stability of an aircraft evaluated, investigation of related stability derivatives is essential as stated previously. Together with similar variables in longitudinal equations, equations of lateral derivatives also include lateral stability coefficients, wing span, x-axis moment of inertia and z-axis moment of inertia variables.

Y-force lateral stability derivatives are Y_p , Y_r and Y_{δ_r} , which refers to variation in Y-force in terms of rudder deflection δ_r and angular velocities p and r . C_{y_p} , C_{y_r} , and $C_{y_{\delta_r}}$ are nondimensional lateral stability coefficients as stated in equations below.

$$Y_p = \frac{QsbC_{y_p}}{2mu_0} \quad (11)$$

$$Y_r = \frac{Q S b C_{y_r}}{2 m u_0} \quad (12)$$

$$Y_{\delta_r} = \frac{Q S C_{y_{\delta_r}}}{m} \quad (13)$$

Lateral stability moment derivatives of L_p , L_r , L_{δ_α} and L_{δ_r} give brief idea about effects of angular velocities p and r , aileron deflection δ_α and rudder deflection δ_r on variation of rolling moment. Moreover, relative stability coefficients are C_{l_p} , C_{l_r} , $C_{l_{\delta_\alpha}}$, $C_{l_{\delta_r}}$ as stated in equations below.

$$L_p = \frac{Q S b^2 C_{l_p}}{2 I_x u_0} \quad (14)$$

$$L_r = \frac{Q S b^2 C_{l_r}}{2 I_x u_0} \quad (15)$$

$$L_{\delta_\alpha} = \frac{Q S b C_{l_{\delta_\alpha}}}{I_x} \quad (16)$$

$$L_{\delta_r} = \frac{Q S b C_{l_{\delta_r}}}{I_x} \quad (17)$$

Lateral-directional stability moment derivatives of N_{δ_r} , N_{δ_α} and N_r give brief idea about effects of angular velocity r , aileron deflection δ_α and rudder deflection δ_r with variation of yawing moment. Similar with previous moment derivatives, nondimensional relative stability coefficients $C_{n_{\delta_r}}$, $C_{n_{\delta_\alpha}}$ and C_{n_r} are included as stated in equations below.

$$N_{\delta_r} = \frac{Q S b C_{n_{\delta_r}}}{I_z} \quad (18)$$

$$N_{\delta_\alpha} = \frac{Q S b C_{n_{\delta_\alpha}}}{I_z} \quad (19)$$

$$N_r = \frac{Q S b^2 C_{n_r}}{2 I_x u_0} \quad (20)$$

2.4. Aerodynamic Investigation

In this paper, aerodynamic investigation of the vehicle was carried out by means of general public licensed computational program, XFLR5. The program includes LLT (lifting line theory), VLM (vortex lattice method) and 3D panel method options within three-dimensional analysis environment, meanwhile capable of carrying out two-dimensional airfoil analyses with admissible accuracy for such a comparative study (Ahmad et. al., 2021).

Analysis environment constructed at sea-level density of 1.225 kg/m^3 and cruise speed of 16.67 m/s . In order to obtain realistic results in terms of parasitic drag, viscous effects were taken into consideration rather than potential flow approximation. Modeled three-dimensional wing models having dihedral angles of 0 , 15 , 30 and 45 degrees from 84.7% semi-span location are represented in Figure 3. It can be clearly seen that wingspan and wing area of the designs having dihedral angle were shortened and correspondingly their aspect ratios, which can be estimated from Equation 21 using wing span and wing area variables, were diminished (Gudmundsson, 2013).

$$AR = \frac{b^2}{S} \quad (21)$$

Multi-panel wings have spanwise-varying dihedral angle, such as wingtip morphing applied wing in this article. Therefore, in this case, it is required for stability and control estimations to determine equivalent dihedral angle (EDA) of total wing. EDA of a polyhedral wing can be estimated by means of locations of different dihedral angle applied sections in terms of their semi-spanwise locations and values of dihedral angles. In case of two panel wing as our application, taking also moment fractions into consideration, EDA can be estimated from Equation 22, where Γ_1 is dihedral angle of unfolded section and Γ_2 is dihedral angle of morphing wingtip applied section (Beron-Rawdon, 1988).

$$EDA = 0.858 * (\Gamma_1) + 0.142 * (\Gamma_2) \quad (22)$$

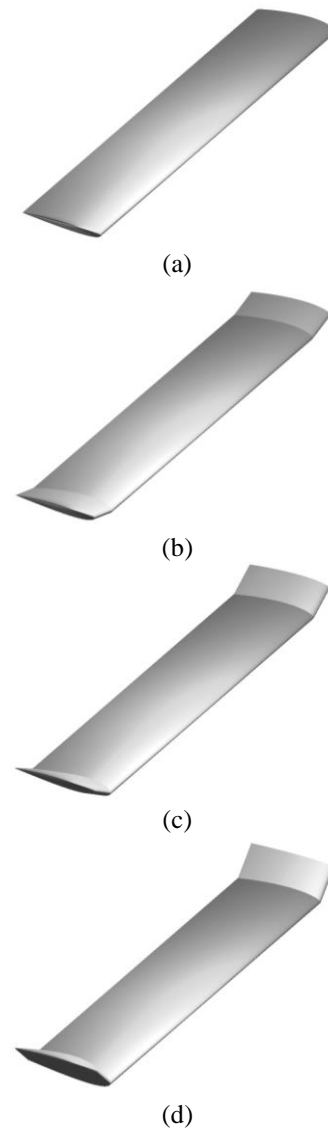


Figure 3. Representative isometric view of ZANKA-I wing design; a) baseline (D0), b) 15-degree morphed wingtip (D15) c) 30-degree morphed wingtip (D30) d) 45-degree morphed wingtip (D45)

3. Results and Discussion

Morphing wingtip application was resulted in morphological changes as expected, and alterations in effective dihedral angle, wing span, wing area, mean aerodynamic chord length and wing aspect ratio due to folding were given in Table 1. Denominations D0, D15, D30 and D45 constructed as abbreviations with respect to wingtip dihedral angles of 0, 15, 30 and 45 degrees, respectively. EDAs for each wing configuration were estimated from Equation 22 and aspect ratios were estimated from Equation 21. The application leads to decrease in wingspan, wing area and wing aspect ratio, while mean aerodynamic chord length remains constant, as expected.

Table 1. Geometrical parameters of ZANKA-I wing design based on morphing wingtip dihedral angle

Parameter	D0	D15	D30	D45
Wingtip Dihedral Angle	0°	15°	30°	45°
Wing Effective Dihedral	0°	2.13°	4.26°	6.39°
Wing Span (m)	1.3	1.293	1.273	1.241
Aerodynamic Chord (m)	0.25	0.25	0.25	0.25
Wing Area (m ²)	0.325	0.323	0.318	0.310
Wing Aspect Ratio	5.2	5.173	5.093	4.966

In order to evaluate stability derivatives, it is required to obtain aerodynamic effects as indicated before. Therefore, computational application of 3D panel method was performed on both base model and configurations with wingtip dihedral. The results of the analyses shown that, increment in wingtip dihedral was led to decrease in span-efficiency, *e*, as expected due to change in direction of locally created lift force, but increase in both of the reference drag and lift coefficients. Furthermore, while D15 has reference lift coefficient of 0.66% higher than D0 configuration, D30 and D45 has 1.4% and 2.25% higher values from base model, respectively. D15, D30 and D45 was found to have 1.23%, 3.18% and 5.93% higher reference drag coefficient values than base model D0, respectively.

Table 2. Oswald efficiency factor, reference lift and drag coefficients with respect to morphing wingtip configuration

Symbol	D0	D15	D30	D45
C_{L_0}	0.6494	0.6537	0.6585	0.6640
C_{D_0}	0.01322	0.01339	0.01365	0.01401
<i>e</i>	1.013	1.005	0.995	0.983

Figure 4 and Figure 5 represents the change in lift coefficient and drag coefficient with respect to wingtip dihedral angle at a range of angle of attack values between -5 to 10 degrees. As dihedral angle of the wingtip was increased, lift curve slope was found to be tended to a slight increase and higher wingtip dihedral configurations were resulted in lower lift coefficients at higher angle of attacks. An opposite tendency was found at angle of attacks lower than approximately 6°. Drag coefficients point of view, minimum value of the term was found to remain approximately constant independent from wingtip dihedral angle alteration. Nevertheless, curve slope of drag coefficient was found in decreasing tendency with higher dihedral angles as seen in Figure 5. The maximum value of aerodynamic

performance parameter lift-to-drag ratio was found to decrease at higher wingtip dihedral angles, where similar tendency was obtained for reference value of the term, as given in Figure 6.

As a consequence of aerodynamic investigation, alteration tendency of aerodynamic parameters due to morphing wingtip application were found in good agreement with similar studies in the literature (Smith et al., 2014).

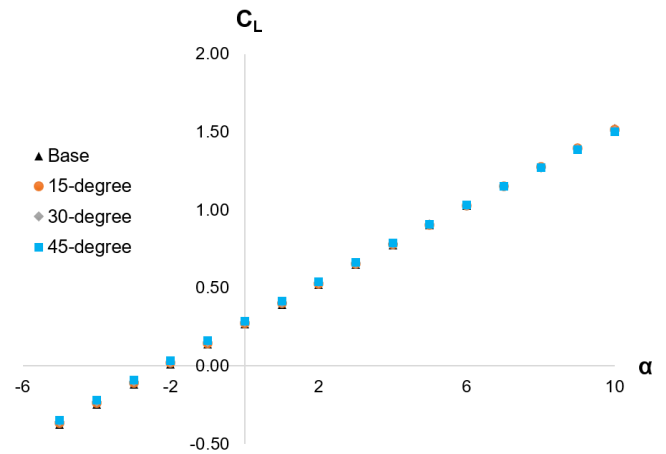


Figure 4. Lift coefficient varying with angle of attack for base model and morphing wingtip configurations of 15, 30 and 45 degrees

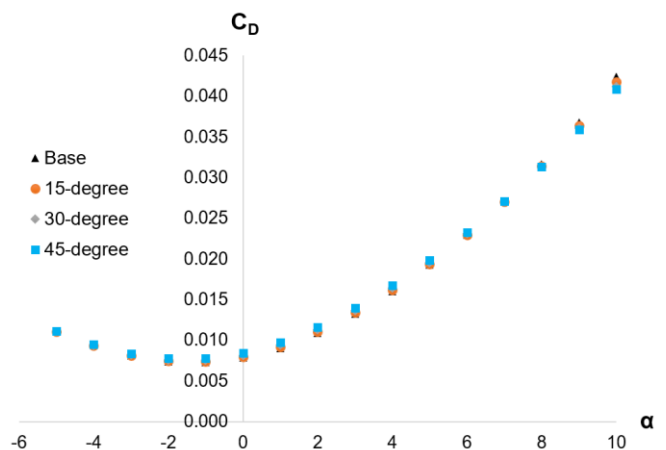


Figure 5. Drag coefficient varying with angle of attack for base model and morphing wingtip configurations of 15, 30 and 45 degrees

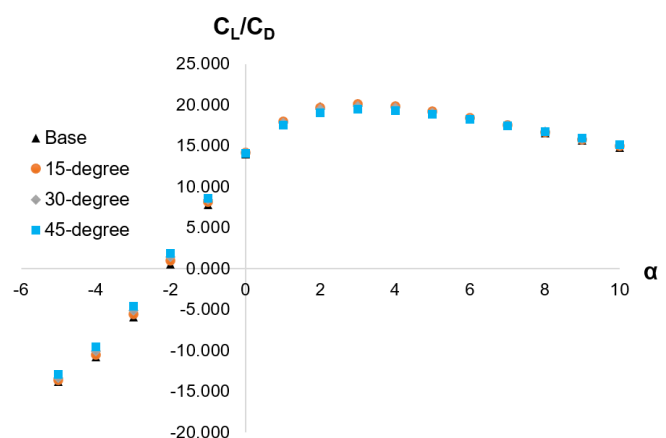


Figure 6. Lift-to-drag ratio varying with angle of attack for base model and morphing wingtip configurations of 15, 30 and 45 degrees

As stated in stability derivative equations, inertial changes have remarkable effect and required to be evaluated. Table 3 gives the resultant moment of inertia values of each configuration for x, y, z axis and also xz plane. It is clear from the table that, while x, z and xz plane moments of inertia were diminished with wingtip dihedral, y moment of inertia oppositely found to increase.

Table 3. Moments of inertia (kgm²) with respect to morphing wingtip configuration

Symbol	D0	D15	D30	D45
I _x	0.09878	0.09843	0.09774	0.09670
I _y	0.14219	0.14330	0.14672	0.15107
I _z	0.22971	0.22892	0.22717	0.22453
I _{xz}	0.01276	0.01269	0.01250	0.01218

Table 4. Longitudinal stability derivative values with respect to morphing wingtip configuration

	D0	D15	D30	D45	Unit
X _u	-0.0602	-0.0606	-0.0608	-0.0609	s ⁻¹
X _w	0.8342	0.8438	0.8416	0.8322	s ⁻¹
Z _u	-1.9697	-1.9722	-1.9560	-1.9232	s ⁻¹
Z _w	-7.3441	-7.3354	-7.2568	-7.1051	s ⁻¹
Z _{δ_e}	-8.0212	-8.0212	-8.0212	-8.0212	ft/s ²
M _w	-1.413	-1.410	-1.381	-1.338	ft.s ⁻¹
M _{ẇ}	-0.0445	-0.0443	-0.0435	-0.0424	ft ⁻¹
M _{δ_e}	-61.491	-61.009	-59.590	-57.874	s ⁻²

Table 5. Lateral-directional stability derivative values with respect to morphing wingtip configuration

	D0	D15	D30	D45	Unit
Y _β	-0.07593	-0.07598	-0.07612	-0.07636	ft/s ²
N _β	0.18152	0.18111	0.17945	0.17666	s ⁻²
L _β	0.00000	-0.62075	-1.09509	-1.31102	s ⁻²
N _p	-2.304	-2.291	-2.218	-2.096	s ⁻¹
L _p	-45.641	-45.263	-43.710	-41.124	s ⁻¹
Y _r	0.002513	0.002513	0.002513	0.002513	ft/s
N _r	-0.035	-0.035	-0.034	-0.032	s ⁻¹
L _r	4.617	4.590	4.445	4.200	s ⁻¹
Y _{δ_r}	0.02675	0.02675	0.02675	0.02675	ft/s ²
N _{δ_i}	-78.932	-80.045	-81.641	-83.634	s ⁻²
N _{δ_i}	-0.159	-0.158	-0.155	-0.149	s ⁻²
L _{δ_c}	706.555	711.842	720.296	731.078	s ⁻²
L _{δ_r}	9.682	9.754	9.870	10.018	s ⁻²

Longitudinal stability derivative results in Table 4 were shown that, D45 configuration found to have 1.16% higher X_u value and 0.23% lower X_w value from baseline model, which are X-force derivatives related with linear velocities. Furthermore, while Z-force derivatives Z_u and Z_w of D45 configuration were found to decrease at the rate of 2.36% and 3.25% than baseline model, there was no any significant change found in Z_{δ_e}. In addition, moment derivative values of D45 configuration M_w, M_{ẇ} and M_{δ_e} were both found to decrease in a rate of 5.28%, 4.66% and 5.88% from baseline model, respectively.

Dihedral effect derivative L_β and roll damping derivative L_p values at various wingtip dihedral angle configurations are given in Table 5. The derivatives were found to diminish with increasing wingtip dihedral angle, which is desired for a laterally stable vehicle. Similarly, increments in cross coupling derivative L_r, roll due to rudder derivative L_{δ_α} and lateral control power derivative L_{δ_r} with increment in wingtip dihedral angle were also desired results for improvement in lateral stability.

Static directional stability derivative N_β was found to be decreased with dihedral angle of wingtip increased, as a tendency in undesired manner. Cross coupling term N_p was found to be improved with positively tendency. Yaw damping term N_r was found to be increased, which is not proper for directional stability point of view. Adverse yaw term N_{δ_α} and rudder power term N_{δ_r} was found to be improved with wingtip dihedral angle increment.

4. Conclusion

Morphing wingtip application was carried out on a fixed-wing unmanned aerial vehicle in terms of dihedral angle with the aim of investigating aerodynamic and corresponding stability derivative impacts of the morphological transformation. In order to have aerodynamic effects of the application evaluated, three configurations with various dihedral angles (15, 30 and 45 degrees) were assessed by means of computational analyses. In addition to these results, variations in moments of inertia were taken into consideration and various longitudinal, lateral and directional stability derivatives were estimated via an analytical approach. Consequently, application of wingtip dihedral angle led most of the lateral stability derivatives to be improved, while static longitudinal stability was diminished. Directional stability point of view, static directional stability loss was appeared, but total directional stability could be said to be improved in terms of other directional stability derivatives. In addition, this study was shown that there is a possibility for improvement in autonomous control of UAVs as a future study.

Ethical approval

Not applicable.

Conflicts of Interest

The authors declare that there is no conflict of interest regarding the publication of this paper.

References

Ahmad, M., Hussain, Z. L., Shah, S. I. A., Shams, T. A. (2021). Estimation of Stability Parameters for Wide Body Aircraft Using Computational Techniques. Applied Sciences, 11(5), 2087.

Ajaj, R. M. (2021). Flight Dynamics of Transport Aircraft Equipped with Flared-Hinge Folding Wingtips. Journal of Aircraft, 58(1), 98-110.

Beron-Rawdon, B. (1988). Dihedral, Model Aviation Magazine.

Cheung, R. C., Rezgui, D., Cooper, J. E., Wilson, T. (2020). Analyzing the dynamic behavior of a high aspect ratio wing incorporating a folding wingtip. In AIAA Scitech 2020 Forum (p. 2290).

- Çelik, H., Oktay, T., Türkmen, İ. (2016). İnsansız Küçük Bir Hava Aracının (Zanka-I) Farklı Türbülans Ortamlarında Model Öngörülmesi Kontrolü ve Gürbüzlük Testi. *Havacılık ve Uzay Teknolojileri Dergisi*, 9(1), 31-42.
- Çoban, S. (2019). Simultaneous tailplane of small UAV and autopilot system design. *Aircraft Engineering and Aerospace Technology*.
- Çoban, S. (2020). Autonomous performance maximization of research-based hybrid unmanned aerial vehicle. *Aircraft Engineering and Aerospace Technology*.
- Deepa, S. N., Sudha, G. (2015). Modeling and approximation of STOL aircraft longitudinal aerodynamic characteristics. *Journal of Aerospace Engineering*, 28(2), 04014072.
- Dussart, G., Yusuf, S., Lone, M. (2019). Identification of In-Flight Wingtip Folding Effects on the Roll Characteristics of a Flexible Aircraft. *Aerospace*, 6(6), 63.
- Gudmundsson, S. (2013). *General aviation aircraft design: Applied Methods and Procedures*. Butterworth-Heinemann.
- Lixin, W. A. N. G., ZHANG, N., Hailiang, L. I. U., Ting, Y. U. E. (2022). Stability characteristics and airworthiness requirements of blended wing body aircraft with podded engines. *Chinese Journal of Aeronautics*, 35(6), 77-86.
- Kanat, Ö. Ö., Karatay, E., Köse, O., Oktay, T. (2019). Combined active flow and flight control systems design for morphing unmanned aerial vehicles. *Proceedings of the Institution of Mechanical Engineers, Part G: Journal of Aerospace Engineering*, 233(14), 5393-5402.
- Konar M. (2019). Redesign of morphing UAV's winglet using DS algorithm based ANFIS model. *Aircraft Engineering and Aerospace Technology*, 91 (9), pp. 1214-1222.
- Konar, M., Turkmen, A., Oktay T., (2020). Improvement of the thrust-torque ratio of an unmanned helicopter by using the ABC algorithm. *Aircraft Engineering and Aerospace Technology*, 92 (8), 1133-1139.
- Konar M., (2020). Simultaneous determination of maximum acceleration and endurance of morphing UAV with ABC algorithm-based model. *Aircraft Engineering and Aerospace Technology*, 92 (1), 579-586.
- Kose, O., Oktay, T. (2020). Simultaneous quadrotor autopilot system and collective morphing system design. *Aircraft Engineering and Aerospace Technology*.
- Kose, O., Oktay, T. (2021). Hexarotor Longitudinal Flight Control with Deep Neural Network, PID Algorithm and Morphing. *European Journal of Science and Technology*, (27), 115-124.
- Nelson, R. C. (1998). *Flight stability and automatic control* (Vol. 2). New York: WCB/McGraw Hill.
- Oktay, T., Konar, M., Onay, M., Aydin, M., Mohamed, M. A. (2016). Simultaneous small UAV and autopilot system design. *Aircraft Engineering and Aerospace Technology*.
- Oktay, T., Celik, H., Turkmen, I. (2018). Maximizing autonomous performance of fixed-wing unmanned aerial vehicle to reduce motion blur in taken images. *Proceedings of the Institution of Mechanical Engineers, Part I: Journal of Systems and Control Engineering*, 232(7), 857-868.
- Oktay, T., Eraslan, Y. (2021). Numerical Investigation of Effects of Airspeed and Rotational Speed on Quadrotor UAV Propeller Thrust Coefficient. *Journal of Aviation*, 5(1), 9-15.
- Schooser, J., Cuadrat-Grzybowski, M., Castro, S. G. (2022). Preliminary control and stability analysis of a long-range eVTOL aircraft. In *AIAA SCITECH 2022 Forum* (p. 1029).
- Smith, D. D., Lowenberg, M. H., Jones, D. P., Friswell, M. I. (2014). Computational and experimental validation of the active morphing wing. *Journal of aircraft*, 51(3), 925-937.
- Sofla, A. Y. N., Meguid, S. A., Tan, K. T., Yeo, W. K. (2010). Shape morphing of aircraft wing: Status and challenges. *Materials & Design*, 31(3), 1284-1292.
- Şumnu, A., Güzelbey, I. H. (2021). CFD Simulations and External Shape Optimization of Missile with Wing and Tailfin Configuration to Improve Aerodynamic Performance. *Journal of Applied Fluid Mechanics*, 14(6), 1795-1807.
- Yen, S. C., Fei, Y. F. (2011). Winglet dihedral effect on flow behavior and aerodynamic performance of NACA0012 wings. *Journal of fluids engineering*, 133(7).

Cite this article: Oktay, T., Eraslan, Y. (2022). Stability Evaluation of a Fixed-wing Unmanned Aerial Vehicle with Morphing Wingtip. *Journal of Aviation*, 6(2), 103-109.



This is an open access article distributed under the terms of the Creative Commons Attribution 4.0 International License

Copyright © 2022 Journal of Aviation <https://javsci.com> - <http://dergipark.gov.tr/jav>